ELSEVIER

Biochimica et Biophysica Acta 1277 (1996) 253–265

BIOCHIMICA ET BIOPHYSICA ACTA
BBA

Quantification of the number of spins in the S_2- and S_3-states of Ca^{2+}-depleted photosystem II by pulsed-EPR spectroscopy

Alain Boussac *

Section de Bioénergétique, URA CNRS 2096, CEA Saclay, 91191 Gif sur Yvette, Cedex, France

Received 8 December 1995; accepted 24 June 1996

Abstract

Ca^{2+}-depletion of the photosystem II enzyme by a NaCl-washing in the light inhibits oxygen evolution. In Ca^{2+}-depleted photosystem II the S_3 charge storage state exhibits a split EPR signal attributed to the magnetic interaction between a radical and the Mn-cluster. Further treatment of photosystem II by EGTA modifies the shape of the EPR signal of the Mn-cluster in the S_2 charge storage state. The percentage of centers in which the S_2 modified signal and the split S_3 signal can be observed has been estimated by using pulsed-EPR spectroscopy. On the basis of one tyrosine D radical per reaction center, the field-swept spin echo spectrum of the modified S_2 state in dark-adapted photosystem II was detected in a large majority of the reaction centers. The derivative of the S_2 field-swept spectrum with respect to the magnetic field resulted in a spectrum similar to that observed by cw-EPR. The additional light-induced split S_3 signal appeared on top of the envelope of the S_2 signal and was detected in the same proportion of centers as that which exhibited the S_2 signal prior to the illumination. In the formal S_3 state, the hyperfine lines of the Mn field-swept echo spectrum were no longer detectable. The storage of PS-II at 77 K after formation of the $S_3Q_A^-$ state by freezing the membranes under continuous illumination resulted in a decrease of the S_3 signal but the pulsed-EPR S_2 manganese signal was conserved.

Keywords: Electron paramagnetic resonance; Oxygen evolution; Mn-complex; Radical–metal interaction

1. Introduction

Photosystem-II (PS-II) catalyzes light-driven water oxidation resulting in oxygen evolution. The reaction center of PS-II is made up of two membrane-spanning polypeptides (D1 and D2) analogous to the L and M subunits of the purple photosynthetic bacterial reaction center (see Ref. [1] for a review). Absorption of a photon leads to a charge separation between a chlorophyll molecule, designated P_{680}, and a pheophytin molecule. The pheophytin anion transfers the electron to a quinone Q_A and P_{680}^+ is reduced by a

Abbreviations: P_{680}, chlorophyll (Chl) center of photosystem II (PS-II); TyrZ, the tyrosine acting as the electron donor to P_{680}; TyrD, the tyrosine acting as a side-path electron donor of PS-II; Q_A, primary quinone electron acceptor of PS-II; EPR, electron paramagnetic resonance; ESEEM, electron spin echo envelope modulation; EGTA, ethylene glycol bis(β-aminoethyl ether)-*N,N,N′,N′* tetraacetic acid; PPBQ, phenyl-para-benzoquinone; Mes, 2-(*N*-morpholino)ethanesulfonic acid; Tris, tris(hydroxymethyl)aminomethane; EDTA, ethylene diamine tetraacetic acid.

* Corresponding author. Fax: +33 169 088717.

PII S0005-2728(96)00107-7

tyrosine residue, TyrZ, tyrosine 161 of the D1 polypeptide [2–4]. A cluster of 4 manganese ions located in the reaction center of PS-II probably acts both as the active site and as a charge accumulating device of the water-splitting enzyme (see Refs. [5,6], for reviews). During the enzyme cycle, the oxidizing side of PS-II goes through five different redox states that are denoted S_n, n varying from 0 to 4 [7]. The oxygen is released during the S_3 to S_0 transition in which S_4 is a transient state. In addition to TyrZ, there is a second redox active tyrosine in PS-II, TyrD, tyrosine 160 of the D2 polypeptide [2,8,9], the radical of which is normally stable in the dark.

Ca^{2+} and Cl^- are two essential cofactors for oxygen evolution [5,10–12]. In Ca^{2+}-depleted and Cl^--depleted PS-II, inhibition of the enzyme cycle occurs at the S_3 to S_0 transition [5,11,13].

The addition, in the presence of light, of a range of chelators (EGTA, EDTA, citrate, pyrophosphate, etc.) during or after the salt-washing procedure done in the light, results in an additional modification of the enzyme, manifested as a major modification of the spectral properties of the S_2-multiline and also as the stabilization of the S_2 state [5,11,14]. Electron spin echo envelope modulation (ESEEM) data were obtained showing hyperfine couplings in the modified S_2 Mn EPR signal which were attributed to nucleus of nitrogen atoms of the EGTA [15]. Evidence for EGTA binding to the Mn cluster has received some support with experiments in which the EGTA effect in Ca^{2+}-depleted PS-II was lost after a further Cl^--depletion followed by a Cl^--reconstitution [16].

Continuous or flash illumination on Ca^{2+}-depleted PS-II induced the formation of the split S_3 EPR signal centered at $g = 2$ with a width of 164 gauss. The appearance of the split S_3 EPR signal is accompanied by the disappearance of the multiline signal in cw-EPR [18] but not by the disappearance of the S_2 manganese signal as detected by field-swept spectra using pulsed EPR [15,19]. These results were explained by a magnetic interaction between the Mn-cluster and an organic free radical formed in the S_2 to S_3 transition [15,17,18]. The assignment of the S_3 state to an oxidized radical led to the proposal that the Mn cluster itself remained in the same redox state as in the S_2 state, although it became undetectable as a cw-EPR multiline signal. This assignment was supported by EPR simulations demonstrating that weak magnetic interactions required for generating the split EPR signal would also lead to the disappearance of the hyperfine lines from the Mn signal [17,18]. Infrared [20] and UV [18] absorption change measurements indicated that this radical could be His$^{\cdot}$ although recent pulsed-ENDOR and ESEEM measurements seem strongly in favor of TyrZ$^{\cdot}$ [21,22].

The strict inverse relationship between the Mn multiline signal and the split S_3 signal [13,17,18] has been questioned [23]. Indeed, storage of samples at low temperature results in a decrease in the split S_3 signal which is not accompanied by a reappearance of the Mn multiline signal in cw-EPR. The decrease of the S_3 signal is presumably due to the reduction of S_3 by electrons coming back from Q_A^-. In the magnetic interaction model as originally postulated [17,18], the multiline signal would be expected to reappear under these conditions.

Our previous quantification of the number of spins in the S_2 and S_3 signals done by pulsed EPR indicated that these two states were observed in almost all the centers [15,19] (i.e., in 85% of the reaction centers since the Ca^{2+}-depletion procedure induced the loss of Mn in the other 15% which therefore behave like Tris-washed PSII [24]). This result, however, together with the conservation of the envelope of the S_2 signal in the field-swept spectrum has been challenged. Two reports indicated that the S_3 state was formed in only 14% to 23% of the centers [21,25] and reported that the broad envelope of the S_2 signal was not conserved after formation of the S_3 signal. The value of 5.6 spins per center in the S_2 state has also been reported [25]. Since submission of the original version this work, the split radical observed in the formal S_3 state has been detected in 50% of acetate-treated PSII reaction centers [26]. In all these studies [21,25,26], quantifications of the number of spin detected in the S_2 state and S_3 state were done by comparison with the TyrD$^{\cdot}$ signal measured in conditions in which 1 TyrD$^{\cdot}$ per reaction center is expected.

In this study, quantification of the number of spins in the S_2 and S_3 signals detected by pulsed-EPR has been reinvestigated using a combination of instrument settings allowing the detection of the TyrD$^{\cdot}$ signal at the same time as the S_2 or S_3 signals. It is shown that the $cytb_{559}$ signal can also be used for the quantification. The results confirm that the S_2 and S_3

signals are formed in the majority of the PS-II centers.

2. Materials and methods

Photosystem II membranes were isolated from spinach as already described [17]. Calcium-depleted, EGTA-treated and polypeptide-reconstituted PSII were prepared as previously described [17]. All the experiments were done in a medium containing 0.3 M sucrose, 25 mM Mes pH 6.5 and 10 mM NaCl. The Ca^{2+}-depleted PS-II membranes were put in quartz EPR tubes and, after dark adaptation for 1 h at 0°C, 1 mM PPBQ (dissolved in dimethyl-sulfoxide) as an artificial electron acceptor, was added. The samples were immediately frozen at 200 K in a CO_2-ethanol bath, then transferred to liquid nitrogen (77 K). Mn depletion of PS-II was done by Tris-washing the PS-II membranes for 30 min, under room light, at 4°C, in 0.8 M Tris (pH 8.5) and 0.1 mM EDTA. Then, the Tris-washed membranes were collected by centrifugation and washed in 0.3 M sucrose, 10 mM NaCl, 10 mM $CaCl_2$ (to remove any adventitious bound Mn^{2+}) and 25 mM Mes (pH 6.5), pelleted again by centrifugation, washed in 0.3 M sucrose, 10 mM NaCl, 25 mM Mes (pH 6.5) and 0.1 mM EDTA, pelleted and re-suspended in the same medium. The sample was then put in an EPR tube, illuminated at 0°C for 1 min, dark-adapted for 30 s and frozen in the dark at 200 K then to 77 K. The pH value of 6.5 for the final re-suspension buffer was used to have the same pH condition as the Ca^{2+}-depleted PS-II and because a better stability of TyrD$^{\cdot}$ at this pH than at pH 8.5 [27].

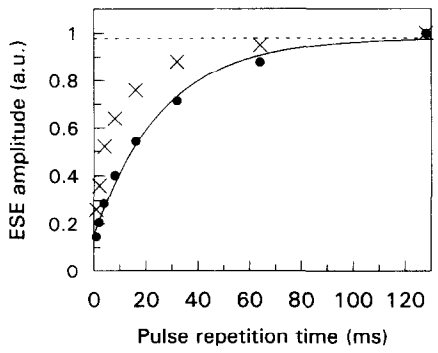

Fig. 1. Electron spin echo amplitude (in arbitrary units) of the TyrD$^{\cdot}$ signal in the Tris-washed sample (closed circles) or of the TyrD$^{\cdot}$ signal in the S_3 state of the Ca^{2+}-depleted PSII (crosses) as a function of the pulse repetition time in a two-pulse sequence $(\pi/2, \tau, \pi)$ at 4.2 K. The duration of the $\pi/2$ and π pulses was respectively 64 ns and 128 ns and the τ-value was 200 ns. The line through the points corresponds to an exponential fitting and the dashed line corresponds to the asymptotic level of the exponential fit.

The maximum amount of TyrD$^{\cdot}$ per reaction center has been reported to be generated in untreated PSII membranes which was illuminated at 0°C for 30 min in the presence of PPBQ [21,26,28]. To apply this protocol, oxygen evolving PSII membranes were washed in 20 mM Tris (pH 8.0), 20 mM NaCl and 0.4 M sucrose and resuspended in the same medium in the presence of 1.5 mM PPBQ. The sample, in the EPR tube, was illuminated for 30 min at 0°C, dark-adapted for 30 s, then frozen at 77 K.

Illumination of the samples was done with a 800-W projector through water and infra-red filters in a non-silvered dewar filled with ethanol and cooled to 0°C with solid CO_2.

CW-EPR spectra were recorded at liquid helium temperatures with a Bruker ER 200D or ESP300 X-band spectrometer equipped with Oxford Instruments cryostats. Pulsed EPR spectra were recorded with a Bruker ESP 380 spectrometer as already described [15]. The field-swept spectra were obtained by measuring the amplitude of the echo as a function of the magnetic field after a two-pulse sequence $(\pi/2, \tau, \pi)$. In experiments done in view of spin quantification, the duration of the $\pi/2$ and π pulses was, respectively, 64 ns and 128 ns and the τ value was 200 ns. The pulse repetition time was 50 ms.

The long pulse repetition time used in this study allows a complete spin relaxation between the pulse-sequences of the fast relaxing species. However, TyrD$^{\cdot}$ which has the slowest spin relaxation among the species studied here could potentially be slightly underestimated even with a pulse repetition time of 50 ms (see Ref. [29]). Fig. 1 shows experiments aimed at evaluating this potential underestimate. The amplitude of the electron spin echo of TyrD$^{\cdot}$, in Tris-washed PSII, is plotted as a function of the pulse repetition time at 4.2 K (closed circles). As a first approximation the experimental points are fitted by an exponential function. The dashed horizontal line in Fig. 1 shows the asymptotic level of the exponential function. For a pulse repetition time of 50 ms the

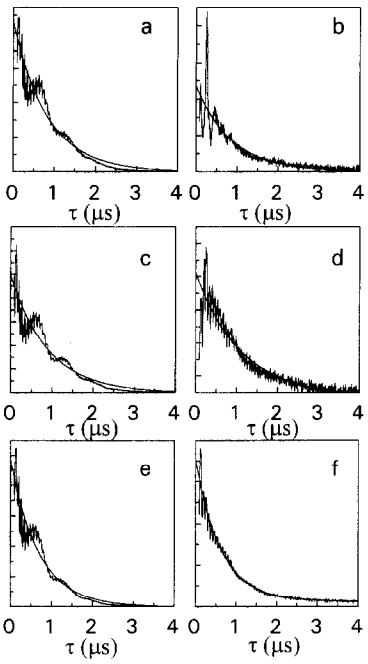

Fig. 2. Electron spin echo amplitude (in arbitrary units) as a function of the τ-value in a two-pulse sequence ($\pi/2$, τ, π) at 4.2 K. The duration of the $\pi/2$ and π pulses was respectively 8 ns and 16 ns and the pulse repetition time was 50 ms. The line through the points corresponds to an exponential fitting. Panels a, TyrD$^{\cdot}$ signal in Tris-washed PSII measured at 3460 gauss; Panel b, cytb_{559} signal in Tris-washed PSII measured at 3520 gauss; panel c, TyrD$^{\cdot}$ signal in the S_2 state of Ca^{2+}-depleted PSII measured at 3460 gauss; Panel d, Mn signal in the S_2 state of Ca^{2+}-depleted PSII measured at 3520 gauss; panel e, TyrD$^{\cdot}$ signal in the S_3 state of Ca^{2+}-depleted PSII measured at 3460 gauss; Panel e, S_3 signal in Ca^{2+}-depleted PSII measured at 3520 gauss.

amplitude of the echo was slightly underestimated by approx. 15%. The crosses in Fig. 1 show the electron spin echo amplitude of TyrD$^{\cdot}$ in the S_3 state of Ca^{2+}-depleted PSII. In this case, the use of a pulse repetition time of 50 ms resulted in an underestimation of TyrD$^{\cdot}$ lower than 10%.

The use of a long pulse duration in the field-swept spin echo experiments can also slightly underestimate the number of spins which correspond to species that have a short phase memory time value (T_M) by comparison with those having a long T_M. The T_M values can be estimated by a 2-pulse sequence [30]. Fig. 2 shows the electron spin echo amplitude of the different species studied here as a function of the τ value of a 2-pulse sequence ($\pi/2$, τ, π). Panels a, c and e show the 2-pulse echo recorded on the TyrD$^{\cdot}$ signal in Tris-washed sample and in the S_2 and S_3 states of the Ca^{2+}-depleted PSII respectively. Panel b shows the 2-pulse echo recorded on the cytb_{559} signal in the Tris-washed sample. Panel d shows the 2-pulse echo recorded on the S_2 signal of Ca^{2+}-depleted PSII. Panel e shows the 2-pulse echo recorded on the S_3 signal of Ca^{2+}-depleted PSII. The T_M values estimated by an exponential function through the experimental points varied between 0.8 μs and 1 μs as follows (see also [15,31]): $T_M(\text{cyt}b_{559}) \approx T_M(\text{TyrD}^{\cdot}) \geq T_M(S_2) \approx T_M(S_3)$. The small variations between the different T_M values and the fact that the T_M values are significantly longer than the pulses length used in the field-swept experiments indicate that the S_2 and S_3 field-swept signals were only very slightly mis-estimated with regard to the cytb_{559} and TyrD$^{\cdot}$ field-swept signals.

In systems in which an electron-electron spin-spin interaction occurs, it has been shown that the relative amplitude of each line, in the field-swept spectrum, depended on their effective spin value S [32]. Indeed, the higher the effective spin value, the lower the microwave power required to flip the spin by 90° with a $\pi/2$ pulse. In the S_3 state, the microwave power required to observed the maximum amplitude of the echo after the two-pulses sequence ($\pi/2 = 64$ ns and $\pi = 128$ ns) was found similar for all the magnetic field positions. This indicates that the estimation of the area of the manganese signal and of the radical signal in the S_3 state was not perturbed by the effect reported in [32]. A second consequence would be that the split radical and the manganese cluster have a similar effective $S = 1/2$ value in the S_3 state.

Another point which could influence the amplitude a field-swept spectrum is the τ value used. Indeed, the envelop modulation of the electron spin echo could result in an underestimation or an overestimation of the echo amplitude depending on whether the τ-value used corresponds to a peak or a trough in the modulation. This point is illustrated in Fig. 3 which shows the electron spin echo signal of TyrD$^{\cdot}$ after a 2-pulse sequence ($\pi/2$, τ, π), with $\pi = 64$ ns and $\pi = 128$ ns (curve a). In the conditions used to record curve a, the modulation corresponding to the free protons (≈ 15 MHz) which is detected in Fig. 2 (panels a, c, e) is almost totally abolished here. This is expected since the pulses length exceed the modu-

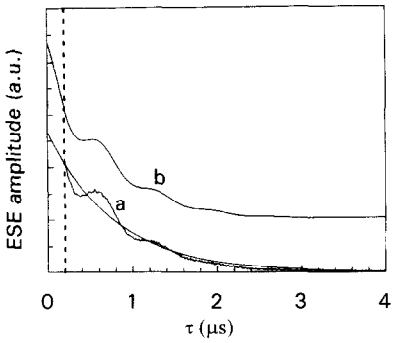

Fig. 3. Curve a: electron spin echo amplitude of the TyrD˙ signal (in arbitrary unit) as a function of the τ-value in a two-pulse sequence ($\pi/2$, τ, π) at 4.2 K. The duration of the $\pi/2$ and π pulses was respectively 64 ns and 128 ns and the pulse repetition time was 50 ms. The line through the points corresponds to an exponential fitting. Curve b shows a theoretical 2-pulse echo of the TyrD˙ signal reconstructed by using a modulation frequency of 1.5 MHz. The vertical dashed line corresponds to the dead-time of the instrument in these conditions.

lation period of the free protons. The line through curve a is an exponential fit of curve a. Curve b in Fig. 3 shows a simulated curve of the TyrD˙ modulations using a frequency of 1.5 MHz. This frequency value of 1.5 MHz was obtained by Fourier transforming curve a. The vertical dashed line is drawn at $\tau = 200$ ns, i.e., the τ value used in the field-swept spectra shown below. It can be concluded that for $\tau = 200$ ns the electron spin echo signal of TyrD˙ has the maximum amplitude which can be measured after the dead-time.

In contrast to TyrD˙, the broad field-swept spectra of the Cytb_{559} signal and of the S_2 and S_3 signals were less affected by the τ-value (not shown). Indeed, the Larmor frequency of a nucleus varies linearly with the magnetic field. For free protons these changes in the Larmor frequency ($\approx$ 15 MHz at 3500 gauss) over a large magnetic field range result in an echo which is alternatively measured on a peak or a trough of the modulation in the case of broad signals. This made critical the choice of a particular τ-value for the recording of field-swept spectra with short pulse duration. Nevertheless, as this is the case for TyrD˙, the long pulse duration used here almost totally abolished the free proton frequency of Cytb_{559} and of S_2 and S_3 (not shown). Since the other modulations are weak (in particular those detected in the cytb_{559}, S_2 and S_3 signals), the choice of a particular τ-value does not significantly influences the field-swept echo spectra.

3. Results and discussion

Quantification of the number of spins in the multiline signal arising from the S_2 state and detected by cw-EPR spectroscopy is difficult. By double integration of the multiline cw-EPR signal Hansson et al. [33] obtained a value of 0.33–0.53 spin/PS-II. Nevertheless, since it was impossible to distinguish the correct baseline of the signal from its envelope, this estimation was not considered as definitive. Since broad signals are easier to detect in pulsed-EPR than in cw-EPR [30], a field-swept spin echo EPR spectrum, roughly equivalent to an absorption spectrum, seems more convenient to estimate the number of spins in the S_2 manganese signal. Absolute quantification of the number of spins can be made by comparison with external standards in which the spin concentration is known. This procedure implies that all the instrument settings are similar both for the sample to study and for the spin standard. This condition is not easily satisfied in pulsed-EPR spectroscopy and may require complicated data treatment. Therefore, the use of internal standards seems more appropriate if their concentration is known. In principal, the signals from cytb_{559} and TyrD˙, can be used to calibrate the number of spins contributing in other PS-II signals.

TyrD˙ is expected to be fully oxidized in Mn-depleted samples prepared by Tris-washing as described in the Section 2. In the literature [21,26,28] it was reported that the yield of TyrD˙ is close to 1 in untreated PSII which were incubated at pH 8 in the presence of an electron acceptor and which were illuminated for 30 min at 0°C. Fig. 4 compares the amplitude of the TyrD˙ signal in untreated PSII after such an illumination (spectrum a), in Tris-washed PSII at pH 6.5 (spectrum b) and in the S_3 state of Ca^{2+}-depleted PSII. The 3 spectra were normalized to the same chlorophyll concentration, i.e., the same reaction center concentration. Spectra b and c have an amplitude similar to spectrum a which corresponds to 1 TyrD˙ per reaction center [21,26,28]. This indicates that the TyrD˙ to reaction center ratio in our Tris-washed and Ca^{2+}-depleted membranes is close to 1

assuming, as it seems likely, the 3 preparations have the same Chl to reaction center ratio.

From the g_z value of the cw-EPR spectrum of cytb_{559}, it can be deduced that the cytochrome is in the low potential form in the NaCl-washed PS-II membranes [17,34] and Mn-depleted membranes (see also Ref. [35] and references therein). The g_Z signal of cytb_{559} is at a magnetic field outside the S_2 and S_3 signals. Therefore, the contribution of the cytb_{559} signal in a complex spectrum can be easily eliminated by first scaling the g_Z signal of cytb_{559} obtained in a Tris-washed sample to that present in the considered spectrum, then by subtracting this calculated cytb_{559} spectrum. One cytb_{559} is present in PS-II membranes from plants [36,37] consequently, when it is fully oxidized, the cytochrome signal corresponds to one spin per reaction center (n.b., in cyanobacteria it has been proposed that 2 copies of cytb_{559} are present [37]).

It has been shown above (Fig. 4) that in samples which are Mn-depleted by a Tris-washing, 1 spin from the TyrD$^{\cdot}$ per reaction center has been detected. Therefore, the TyrD$^{\cdot}$ signal can be used as a standard to calibrate the number of spins in the cytb$_{559}$ signal and in the S_2 and S_3 signals. This was done by comparing the integrated area of the signal from S_2 and S_3 and cytb_{559} to that of the signal from TyrD$^{\cdot}$ measured both in Ca^{2+}-depleted and Tris-washed samples.

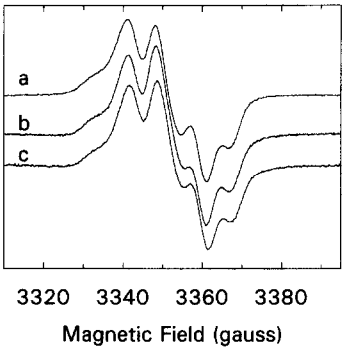

Fig. 4. cw-EPR spectra of the TyrD$^{\cdot}$. Spectrum a was measured in untreated PSII incubated at pH 8 and after illumination for 30 min at 0°C in the presence of PPBQ and a further dark-adaptation of 20–30 s. Spectrum b was recorded in a Tris-washed sample. Spectrum c was recorded in the S_3 state of a Ca^{2+}-depleted PSII. Instrument settings: temperature 15 K; microwave frequency, 9.43 GHz, modulation amplitude 2.8 gauss; modulation frequency, 100 KHz; microwave power, 0.63 μW.

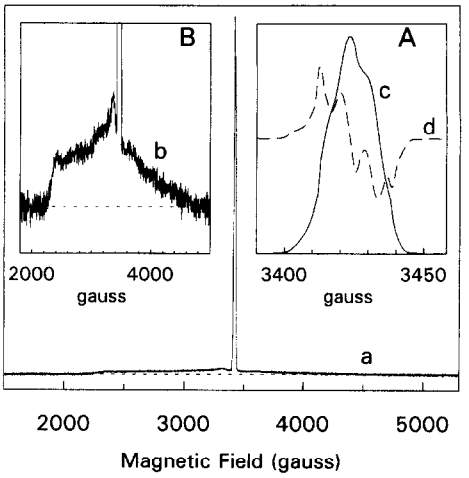

Fig. 5. Spectrum a: Field-swept spin echo spectrum of Tris-washed PS-II. Instrument settings: The amplitude of the echo was measured as a function of the magnetic field after a two-pulse sequence ($\pi/2$, τ, π); the duration of the $\pi/2$ and π pulses was respectively 64 ns and 128 ns and the τ-value was 200 ns; the shot repetition time was 50 ms; temperature, 4.2 K; microwave frequency, 9.6 GHz; magnetic field resolution, 3800 points/3800 gauss. Spectra b and c correspond to spectrum a on different expanded scales. Spectrum d is the first derivative of spectrum c with respect to the magnetic field.

Fig. 5 shows the field-swept spin echo spectrum of a Tris-washed sample. The instrument settings used allowed the cytb_{559} and TyrD$^{\cdot}$ to be recorded simultaneously in the same spectrum. The long pulse duration was required to resolve the hyperfine couplings of TyrD$^{\cdot}$. Inset A in Fig. 5 shows, on an expanded scale, the TyrD$^{\cdot}$ field-swept spin echo spectrum together with its first mathematical derivative with respect to the magnetic field. The hyperfine couplings which are resolved in the TyrD$^{\cdot}$ signal and which are obtained by this procedure are similar (although slightly better resolved) to those which are observed by cw-EPR [38,39] (see Fig. 4 for a comparison). This indicates that no distortion of the TyrD$^{\cdot}$ signal occurred due to improper shot repetition time or pulse duration. Inset B (Fig. 5) shows the cytb_{559} signal on an expanded scale. The g_z signal at $\approx$ 2300 gauss and the g_y signal at $\approx$ 3100 gauss are both resolved. By integrating (i) the whole signal (spectrum a in Fig. 5), (ii) the TyrD$^{\cdot}$ signal (in spectrum a of Fig. 5) after subtraction of the underlying cytb_{559} signal and (iii) the cytb_{559} signal (in spectrum a of Fig. 5) after subtraction of the overly-

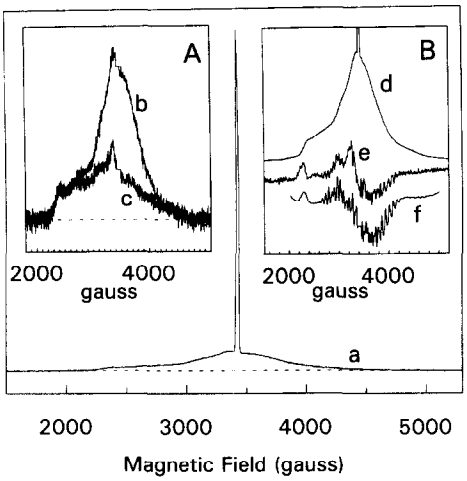

Fig. 6. Spectra a and d: Field-swept spin echo spectra of Ca^{2+}-depleted, EGTA-treated and polypeptide-reconstituted PS-II in the dark-adapted S_2 state. Spectrum b corresponds to spectrum a on a different vertical scale (the TyrD$^{\cdot}$ signal has been deleted). Instrument settings for spectrum a are similar to those used in Fig. 5. Spectrum c is a replot of spectrum a in Fig. 5 and is normalized to spectrum b by adjusting the g_z signal of cytb_{559}. Spectrum d was recorded with the same instruments settings except the number of accumulations which was 25 times greater ($\approx$ 22 h). Spectrum e is the first derivative of spectrum d with respect to the magnetic field. Spectrum f, cw-EPR spectrum of Ca^{2+}-depleted, EGTA-treated and polypeptide-reconstituted PS-II in the dark-adapted S_2 state. Instrument settings: temperature 10 K; microwave frequency, 9.43 GHz, modulation amplitude 22 gauss; modulation frequency, 100 KHz; microwave power, 20 mW.

ing TyrD$^{\cdot}$ signal, it can be found that the area of the TyrD$^{\cdot}$ and cytb_{559} signals contribute for 52% and 48%, respectively, of the total area of spectrum a. This results in the following ratio: cytb_{559}/TyrD$^{\cdot}$ $\approx$ 0.92. On the basis of 1 TyrD$^{\cdot}$ per reaction center (Fig. 4) and since the TyrD$^{\cdot}$ signal was underestimated by $\approx$ 15% (see Fig. 1), it can be estimated that the cytb_{559} was oxidized in 78% (i.e., 0.85 $\times$ 92) of the Tris-washed reaction center.

The S_2 manganese signal was recorded by pulsed-EPR with instrument settings similar to those used in Fig. 5. Fig. 6 (spectrum a) shows the field-swept spin echo spectrum of the dark-adapted Ca^{2+}-depleted PS-II which corresponds to the signals recorded in the S_2 state. Inset A in Fig. 6 (spectrum b) shows the broad signal underlying the TyrD$^{\cdot}$ signal and a cytb_{559} spectrum (spectrum c) recorded in a Tris-washed sample. Spectrum c has been normalized to spectrum b by scaling the amplitude of the g_z signal of cytb_{559}. This procedure is justified since the g_z values of the cytb_{559} signal were found similar both in the Tris-washed sample and the Ca^{2+}-depleted sample. This interactive scaling allows an estimation of the intensity of the cytb_{559} signal in the spectrum recorded in the S_2 state of the Ca^{2+}-depleted sample.

Integration of (i) the whole spectrum a, (ii) the TyrD$^{\cdot}$ signal alone (in spectrum a) after subtraction of the underlying spectrum, and (iii) spectrum a after the removal of the overlying TyrD$^{\cdot}$ signal, gives the following ratio: $(S_2 + \text{cyt}b_{559})/\text{TyrD}^{\cdot} \approx 2.33$. Integration of spectra b and c gives the following ratio $S_2/\text{cyt}b_{559} \approx 0.9$. Taken together, these results give the following ratio: TyrD$^{\cdot}$/S_2/cytb_{559} $\approx$ 0.82/0.9/1.

In a previous pulsed-EPR study of the oxygen evolving enzyme, it has been shown that the first derivative of the signal from S_2 in untreated PS-II with respect to the magnetic field was comparable to that obtained by cw-EPR [31]. A possible criticism [21] of our earlier field-swept echo studies is that the broad S_2 signal detected by this method may not correspond to the multiline signal [15]. In Fig. 6B a field-swept spin echo spectrum of the S_2 state in Ca^{2+}-depleted PS-II membranes has been recorded in the same conditions used for spectrum a in Fig. 5 but with a larger number of accumulations (spectrum d, inset B of Fig. 6). Spectrum e (Fig. 6) is the first derivative of spectrum d with respect to the magnetic field and spectrum f is the cw-EPR signal of the S_2-state. The similarity between spectra e and f shows that the broad signal in field-swept spin echo measurements arises from the Mn complex in the modified S_2 state on top of the cytb_{559} signal.

Quantification of the number of spins in the S_3 signal induced in Ca^{2+}-depleted PS-II by a 0°C illumination indicated that this signal was formed in the same proportion of centers which exhibited the S_2 signal prior to the illumination [15,19]. This quantification is reinvestigated here with the same procedure as above. Fig. 7 (Panel A) shows the field-swept spin echo spectrum of the S_3 state formed in Ca^{2+}-depleted PS-II (spectrum c). This spectrum is plotted together with a replot, taken from Fig. 6, of the S_2 manganese signal (spectrum b). Spectra b and c are normalized to the g_z value of the cytb_{559} signal. Since no change in the redox state of cytb_{559} was

observed during the S_2 to S_3 transition, as detected by cw-EPR (inset of panel A, Fig. 7), and since the g_z signal is outside the S_2 and S_3 signals, this normalization procedure is justified. Spectrum a in panel A of Fig. 7 shows a $cytb_{559}$ signal scaled to spectra b and c with the g_z signal. It can be seen that the broad envelope of the S_2 signal did not disappear after formation of the S_3 signal.

Panel B of Fig. 7 shows the first derivative of the S_3 spectrum with respect to the magnetic field. This derivative signal exhibits the split S_3 signal observed

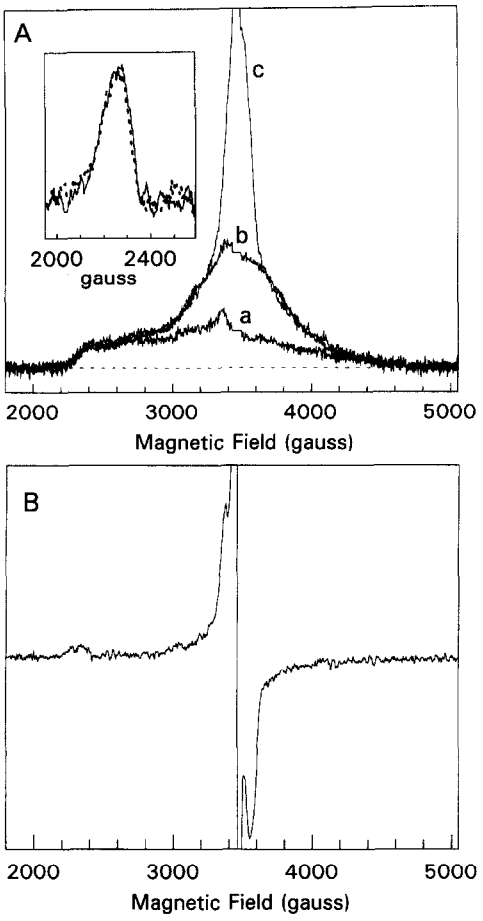

Fig. 7. Panel A, Spectrum c was recorded after a 0°C illumination of Ca^{2+}-depleted, EGTA-treated and polypeptide-reconstituted PS-II. Spectrum a, replot of spectrum a in Fig. 5. Spectrum b, replot of spectrum a in Fig. 6. Same instrument settings as in Fig. 5. The center parts corresponding to the TyrD$^{\cdot}$ signal have been deleted. The inset of panel A shows the g_z signal of the cytb_{559} recorded by cw-EPR in the S_2 state (continuous line) of in the S_3 state (dashed line). Instrument settings as for spectrum f in Fig. 6. Panel B shows the first derivative of spectrum c in panel A with respect to the magnetic field.

Table 1
Estimates of the number of spin of the different species present in Tris-washed PSII and in Ca^{2+}-depleted PSII

	Tris-washed	Ca^{2+}-depleted S_2 state	Ca^{2+}-depleted S_3 state
TyrD$^{\cdot}$	1 [b]	0.70 [f]	1 [b]
cytb_{559}	0.78 [c]	0.85 [e]	0.85 [d]
Mn signal [a]		0.81 [f]	0.80 [d]
split S_3 radical			0.82 [d]

[a] Attributed to S_2 as a modified multiline and in S_3 as the same state lacking the hyperfine lines. [b] Estimated by cw-EPR by comparison, on a Chl concentration basis [21], to a sample reported as to possess 1 TyrD$^{\cdot}$ per reaction center. [c] Compared to TyrD$^{\cdot}$ in the same sample and calculated by using an underestimation of 15% for the amplitude of the field-swept echo TyrD$^{\cdot}$ signal (i.e., $0.78 = 0.85 \times (\text{cyt}b_{559}/\text{TyrD}^{\cdot})$. [d] Compared to TyrD$^{\cdot}$ in the same sample and calculated by using an upper limit of 10% for the underestimation of the amplitude of the field-swept echo TyrD$^{\cdot}$ signal. [e] Normalized to cytb_{559} in the S_3 state (the amplitude of the g_z signal of cytb_{559} is identical in S_2 and S_3 in these samples as monitored by cw-EPR), is also consistent with estimate of $\approx$ 15% photooxidizable cytb_{559} upon illumination at 77 K. [f] Compared to cytb_{559} in the same sample.

in cw-EPR. Moreover, the hyperfine lines of the S_2 signal are no longer detectable after formation of the split radical, as observed in cw-EPR in the same conditions [17].

From Fig. 7, Panel A, integration of (i) spectrum c (which contains the cytb_{559}, the S_2 signal and the light-induced split signal), (ii) the overlying TyrD$^{\cdot}$ signal (not shown in Panel A, Fig. 7), and (iii) spectra a and b, gives the following ratio: cytb_{559}/S_2/split S_3 signal/TyrD$^{\cdot}$ $\approx$ 0.95/0.89/0.92/1.

All the results are summarized in Table 1. According to the literature [21,26,28], and from the results in Fig. 4, 1 TyrD$^{\cdot}$ per reaction center is present in the Tris-washed sample and in the S_3 state of the Ca^{2+}-depleted PSII. From results in Fig. 1, the amplitude of the field-swept signal of TyrD$^{\cdot}$ was underestimated by $\approx$ 15% in the Tris-washed sample and by a maximum of 10% in the Ca^{2+}-depleted PSII. Therefore the values reported in Table 1 take into account this underestimation in the spin count of the other species which were ratioed to the TyrD$^{\cdot}$ signal. The values reported in Table 1 for the S_2 state are normalized to those obtained in the S_3 state by using the cytb_{559} signal amplitude as a reference between both

states (see above). In the S_2 state, the value lower than 1 for the TyrD$^{\cdot}$ signal arises from a proportion of centers ($\approx 30\%$) in which the tyrosine D is reduced (see Ref. [40]), presumably during the dark adaptation. It was also previously shown that calcium depletion leads to an irreversible inhibition in a small proportion of centers (10–15%) in which the multiline signal is not present [24]. This could explain the value of 0.81 for the S_2 signal. Table 1 also shows that the ctyb_{559} is not oxidized in $\approx$ 15–20% of the Ca^{2+}-depleted PSII. This percentage of reduced cytochrome is in agreement with the proportion of the cytb_{559} signal which was formed by a 77 K illumination as detected by cw-EPR (not shown). In samples in which the amount of reduced cytb_{559} is larger than in the preparations used in this study (i.e., $\gg$ 15%) an increased of the cytb_{559} signal can be observed mainly after a long period of illumination at 0°C and at temperatures below 0°C.

The results indicate that the S_3 signal is observed in all the centers in which the modified S_2 signal was present prior to the illumination. This agrees with our earlier studies using different basis for quantification [15,19]. However, it disagrees with reports in which the S_3 signal was found in 23% [25] to 15% [21] of the PS-II centers by using a similar approach to that used here (i.e., taking TyrD$^{\cdot}$ as an internal standard). In addition, our quantification of the S_2 manganese signal, here and earlier [15,19], in Ca^{2+}-depleted PS-II and found close to one per reaction center, differs greatly from that obtained by Gilchrist et al. [25] who found 5.6 spins per reaction. The low value for S_3 and high value for S_2 were made on PSII which were depleted of Ca^{2+} by a treatment using low pH and citrate. Given that the present data used essentially the same method and criteria for quantifications, it seems likely that the discrepancy lies in the different biochemical preparations used. Indeed, preliminary results using a procedure totally identical to that described above and obtained with our citrate-treated PSII [41] indicate that the S_3 signal is about two times smaller than in the NaCl-EGTA-treated material (not shown).

A reviewer raised the possibility that the field-swept signal, which we attribute to the Mn-cluster in a spin $S = 1/2$ state but without the hyperfine lines, might be due to some kind of MnII contamination. This seems unlikely for the following reasons: (1) the broad Mn signal is observed with membranes dialyzed a long time; (2) the same results were observed reproducibly from preparation to preparation over several years in the presence or the absence of a chelator [15,19]; (3) no (or very little) MnII signal, which may be broad at 9 GHz, were detected in such samples at 90 GHz or at 245 GHz which are conditions in which MnII is very easily measured (Sun et al., unpublished).

The question of MnII contaminations seems more likely to be a problem in citrate-treated PSII. Indeed, the citrate-treated preparation is known to be susceptible to the loss of some Mn from the Mn cluster [42]. The MnII (spin 5/2) contamination might be expected to result in anomalous S_2 to S_3 ratios (up to 40:1 from Refs. [21] and [25]) and to result in a lower S_3 yield. In the presence of citrate, the released Mn^{2+} ions form a citrate-Mn^{2+} complex. Fig. 8 shows the cw-EPR spectrum of a solution containing 50 μM Mn^{2+} and 20 mM citrate (spectrum a). Spectrum b shows the cw-EPR spectrum of a Tris-washed PS-II sample (at about 20 μM PS-II) in the presence of 50 μM Mn^{2+} and 20 mM citrate. It can be seen that this very large contamination by the citrate-Mn^{2+} complex is hardly detectable in spectrum b. Therefore any contamination of a preparation by a citrate- Mn^{2+} complex will be difficult to detect in a cw-EPR spectrum, especially in samples containing other signals such as the S_2 multiline signal. By contrast, Fig. 8 (spectrum c) shows that, as for the EDTA-Mn^{2+} complex, the citrate-Mn^{2+} complex exhibits a strong field-swept spin echo spectrum. Spectrum c exhibits some similarities to the cytb_{559} signal in Tris-washed PS-II (spectrum d) and the S_2 signal which may make its identification difficult.

It has also been reported that the envelope of the S_2 signal disappeared concomitantly with S_3 formation in citrate-treated material [25]. This observation is also in contradiction with our observation that the envelope of the pulsed-EPR spectrum measured in the S_2 state did not disappear when S_3 was formed ([15,19], this work). Attempting to explain this discrepancy we have added a citrate-Mn^{2+} complex to Tris-washed PS-II membranes and the field-swept spin echo spectrum has been measured before (Fig. 8, spectrum e) and after (Fig. 8, spectrum f) a 0°C illumination of the sample (i.e., the conditions used to generate the S_3 signal). Fig. 8 shows that illumina-

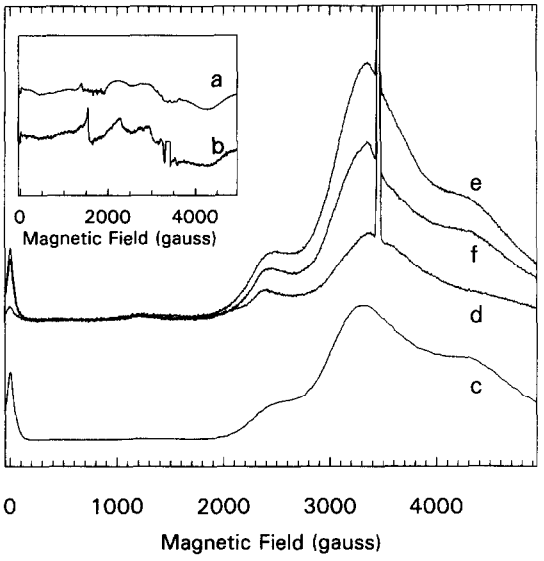

Fig. 8. Spectrum a: cw-EPR spectrum of a solution containing 50 μM Mn^{2+} and 20 mM citrate (pH 6.5). Spectrum b: Tris-washed PS-II (4 mg Chl/ml, i.e., 20 μM of PS-II) in the presence of 50 μM Mn^{2+} and 20 mM citrate (pH 6.5). Instrument settings: temperature 10 K; microwave frequency, 9.43 GHz, modulation amplitude 22 gauss; modulation frequency, 100 kHz; microwave power, 20 mW. Spectrum c: field-swept spin echo spectrum of a solution containing 50 μM Mn^{2+} and 20 mM citrate (pH 6.5). Spectrum d: field-swept spin echo spectrum of Tris-washed PS-II. Spectra e and f were recorded respectively before and after a 0°C illumination of Tris-washed PS-II in the presence of 50 μM Mn^{2+}, 20 mM citrate (pH 6.5) and 1 mM PPBQ. Instrument settings: The amplitude of the echo was measured as a function of the magnetic field after a two-pulse sequence ($\pi/2$, τ, π); the duration of the $\pi/2$ and π pulses was respectively 8 ns and 16 ns and the τ-value was 200 ns; the shot repetition time was 16 ms; temperature, 4.2 K; microwave frequency, 9.7 GHz; magnetic field resolution, 1000 points/5000 gauss.

tion of the sample results in a decrease of the intensity of the citrate-Mn^{2+} signal. This presumably results from electron donation of citrate-Mn^{2+} to Tris-washed PS-II which consequently forms a citrate-Mn^{3+} complex not EPR-detectable. After dark-adaptation, for 30 min at 0°C following the illumination approx. 40% of citrate-Mn^{2+} signal suppressed by the illumination was restored (not shown).

The citrate-MnII properties fulfills all of the characteristics required to explain the phenomenon reported earlier [21,25]. Although other explanations are not eliminated, it seems reasonable to suggest similar effects may be at least partly responsible for the discrepancy seen between the two different biochemical preparations used. It has been previously reported that a long period of illumination at 0°C resulted in a decrease in the intensity of the S_3 signal [40]. It could be possible that the citrate-treated material is more susceptible to the length of the illumination which would result in an apparent low yield in S_3 formation. [1]

Another way to measure the evolution of the field-swept spectrum of S_2 after S_3 formation is derived from the following observation. Storage at 77 K of samples which were frozen under continuous illumination results in a decrease of the split S_3 signal which was not accompanied by a reappearance of the Mn multiline signal as detected by cw-EPR [23]. Fig. 9A shows a similar experiment in which our Ca^{2+}-depleted material was frozen under continuous illumination. Spectrum a corresponds to the dark-adapted state. It exhibits the modified Mn multiline signal, between 2400 and 4200 gauss, characteristic of the stable S_2-state in the Ca^{2+}-depleted, EGTA-treated and polypeptide-reconstituted PS-II. Illumination for 20 s, in the presence of PPBQ, at 0°C results in the characteristic split EPR signal (spectrum b) with a peak-to-trough of 164 gauss and centered at $g = 2$ (3350 gauss) [2]. Freezing of the sample to 77 K under continuous illumination, in the absence of PPBQ, resulted in the formation of the $S_3Q_A^-$-state (not shown). The amplitude of the S_3

[1] It has been discussed [26] that (i) in flash experiments, the yield of the formation of the S_3 signal was lower in Ca^{2+}-depleted PS-II [18] than in acetate-treated PS-II [26] and that (ii) this lower yield was due to a long delay between flashes (1 s, [18]) resulting in S_3 decay in a fraction of the reaction centers. These two assertions are inexact. First, in Ca^{2+}-depleted PS-II [18], the yield of S_3 formation after the first flash was 60%, which is comparable to the 60–65% found in acetate-treated PS-II [26]. Second, in Ca^{2+}-depleted PS-II, this lack of S_3 formation after the flash in 40% of the reaction centers has been shown to be due to similar kinetics for the electron donation from TyrZ to P_{680}^+ and the electron donation from Q_A^- to P_{680}^+ [24]. In Ca^{2+}-depleted PS-II, the S_3 signal decays at room temperature with a $t_{1/2}$ equal to 120 s [40].

[2] The possibility that the S_3 signal arises from OH$^\cdot$ was recently suggested [43]. This was based on the similarity of the g-value of OH$^\cdot$ ($g = 2.011$) and the g-value of a simulated S_3 signal ($g = 2.009$, [18]). The exact g-values of the peak and trough of the split signal are 2.054 and 1.955 respectively. The center of the signal has therefore a g-value equal to 2.0035 ± 0.0010. This value is very different from the g-value of OH$^\cdot$.

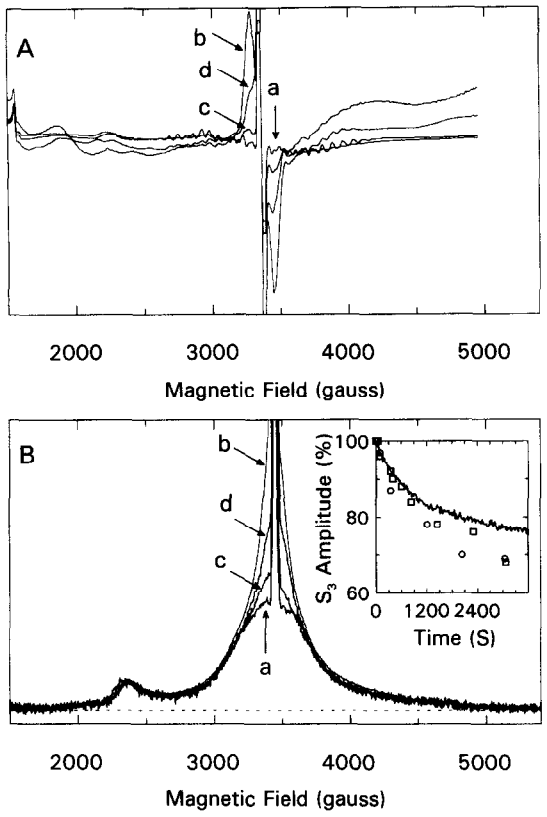

Fig. 9. Panel A: cw-EPR spectra; instrument settings as in Fig. 6B. Panel B: Field-swept spin echo spectra, instruments settings as in Fig. 8. Spectra a were recorded on PS-II dark-adapted at 0°C, i.e., in the S_2 state. Spectra b were recorded after a 0°C illumination in the presence of PPBQ, i.e., in the S_3 state. Spectra c were recorded on samples stored for 9 days at 77 K after freezing under continuous illumination in the absence of PPBQ. Spectra d were recorded after illumination of the sample in the EPR cavity (at 10 K for cw-EPR and 4.2 K for pulsed-EPR) immediately after the recording of spectra c. The distorted baseline in the cw-EPR spectra c and d is due to the oxygen trapped during the storage in liquid nitrogen. To avoid warming of the sample, removal of condensed O_2 by warming to 200 K was not possible after storage in liquid N_2. Different batches of samples were used for experiments reported in panel A and Panel B. Inset of Panel B: Kinetics of the decay in the dark of the S_3 signal formed by illumination in the EPR cavity at 20 K (open circles), 10 K (open squares) and 4.2 K (continuous trace). 100% refers to the amplitude of the S_3 signal just after the illumination in the EPR cavity. The symbols were obtained by cw-EPR measurements and the continuous trace by pulsed-EPR measurements.

signal formed in these conditions was about 70% of that of the S_3 signal formed in the presence of PPBQ. Spectrum c was recorded on a sample frozen under continuous illumination then stored 9 days at 77 K. Spectrum d was recorded after illumination in the EPR cavity at 10 K. As observed previously [23], the S_3 signal disappeared (spectrum c) without the reappearance of the multiline signal. A proportion of TyrD$^{\cdot}$ ($\approx$ 30%) has also disappeared during the storage at 77 K (not shown). S_3 and TyrD$^{\cdot}$ were reduced by a recombination with Q_A^- as indicated by a corresponding decrease of the Q_A^- signal (not shown). As already reported, illumination directly in the EPR cavity between 4.2 and 20 K is able to regenerate 70% of the S_3 signal trapped before storage in liquid N_2, i.e., about 50% of the total S_3 signal (spectrum d). The S_3 state light-induced at helium temperature decreased quickly [23], inset of Fig. 9B). Fig. 9B shows a similar experiment in which spectra were measured by pulsed-EPR. Spectrum c was recorded after storage at 77 K and spectrum d was recorded after illumination at 4.2 K in the pulsed-EPR resonator. A comparison of these spectra can be done with those of a sample in the dark-adapted S_2 state (spectrum a) or in the S_3 state after illumination at 0°C (spectrum b). The stability of the S_3 field-swept signal formed by illumination at 4.2 K is also plotted in the inset of Fig. 9B (continuous line) and resembles that measured by cw-EPR. Examination of Fig. 9B shows that the envelope of the S_2 signal is conserved after the deactivation of S_3 into S_2. This indicates that it is the radical which recombines with Q_A^- and that the Mn-cluster remains in the same redox state, probably S_2. As formation of the S_3 state was done by illumination of the sample in the EPR cavity, conservation of the envelope of the S_2 signal in the S_2 to S_3 transition is real and not due to any modification in the position of the tube nor in the instrument settings.

To explain the lack of the cw-EPR multiline signal upon decay of the S_3 split radical upon storage at low temperature, we suggested that the Mn cluster rather that the radical might be reduced by Q_A^- under these conditions [13]. The experiments shown here indicate that it is not the case. It seems the radical and not the Mn is reduced under these conditions. We must modify our previous hypothesis concerning the disappearance of the cw-EPR multiline signal in the S_3 state. The loss of the hyperfine lines is not due to a direct magnetic effect of the radical but to a secondary effect on the environment of the Mn induced by the presence of the radical. This secondary effect

is temperature-dependent since the hyperfine lines are restored by a warming of the sample at 200 K [23].

4. Conclusion

The instrument settings used in this work allowed the detection in the same spectrum of the cyt b_{559} signal, the S_2 or S_3 signal and the TyrD$^{\cdot}$ signal. All the values are summarized in Table 1. The main conclusion which can been drawn is that the S_2 and S_3 signals are formed in the large majority of the PS-II centers in material Ca^{2+}-depleted by NaCl-washing in the light. A similar conclusion has already been made from the inverse relationship between S_2 and S_3 [17,18] and quantification of the number of spins [15,26]. The broad field-swept spectrum observed in the S_2 sate is shown to arise from the Mn complex since its first derivative with respect to the magnetic field is similar to the S_2 multiline signal as recorded by cw-EPR.

Acknowledgements

The author thanks C. Berthomieu, Y. Deligiannakis, T. Mattioli, S. Un and in particular Bill Rutherford for helpful discussions and suggestions.

References

[1] Michel, H. and Deisenhofer, J. (1988) Biochemistry 27, 1–7.
[2] Barry, B.A. and Babcock, G.T. (1987) Proc. Natl. Acad. Sci. USA 84, 7099–7103.
[3] Debus, R.C., Barry, B.A., Sithole, I., Babcock, G.T. and McIntosh, L. (1988) Biochemistry 27, 9071–9074.
[4] Metz, J.G., Nixon, P.J., Rögner, M., Brudvig, G.W. and Diner, B.A. (1989) Biochemistry 28, 6960–6969.
[5] Debus, R.C. (1992) Biochim. Biophys. Acta 1102, 269–352.
[6] Rutherford, A.W. (1989) Trends Biochem. Sci. 14, 227–232.
[7] Kok, B., Forbush, B. and McGloin, M. (1970) Photochem. Photobiol. 11, 457–475.
[8] Debus, R.C., Barry, B.A., Babcock, G.T. and McIntosh, L. (1988) Proc. Natl. Acad. Sci. USA 85, 427–430.
[9] Vermaas, W.F.J., Rutherford, A.W. and Hansson, Ö. (1988) Proc. Natl. Acad. Sci. USA 85, 8477–8481.
[10] Homann, P.H. (1987) J. Bioenerg. Biomembr. 19, 105–123.
[11] Rutherford, A.W., Zimmermann, J.-L. and Boussac, A. (1992) In The photosystems: Structure, Function and Molecular Biology (J. Barber, ed.), pp. 179–229. Elsevier, Amsterdam.
[12] Yocum, C.F. (1991) Biochim. Biophys. Acta 1059, 1–15.
[13] Boussac, A. and Rutherford, A.W. (1994) Biochem. Soc. Trans. 22, 352–358.
[14] Boussac, A., Zimmermann, J-L. and Rutherford, A.W. (1990) FEBS Lett. 277, 69–74.
[15] Zimmermann, J-L., Boussac, A. and Rutherford, A.W. (1993) Biochemistry 32, 4831–4841.
[16] van Vliet, P., Boussac, A. and Rutherford, A.W. (1994) Biochemistry 33, 12998–13004.
[17] Boussac, A., Zimmermann, J.-L. and Rutherford, A.W. (1989) Biochemistry 28, 8984–8989.
[18] Boussac, A., Zimmermann, J.-L., Rutherford, A.W. and Lavergne, J. (1990) Nature 347, 303–306.
[19] Boussac, A. (1995) Chem. Phys. 194, 409–418.
[20] Berthomieu, C. and Boussac, A. (1995) Biochemistry 34, 1541–1548.
[21] Gilchrist, Jr. M.L., Ball, J.A., Randall, D.W. and Britt, R.D. (1995) Proc. Nat. Acad. Sci. USA 92, 9545–9549.
[22] Tang, X.-S., Randall, D.W., Ann Force, D., Diner, B.A., and Britt, R.D. (1995) J. Am. Chem. Soc., in press.
[23] Hallahan, B.J., Nugent, H.A., Warden, J.T. and Evans, M.C.W. (1992) Biochemistry 31, 4562–4573.
[24] Boussac, A., Sétif, P. and Rutherford, A.W. (1992) Biochemistry 31, 1224–1234.
[25] Gilchrist, M.L., Lorigan, G.A. and Britt, R.D. (1992) In Research in Photosynthesis (Murata, N., ed.), Vol. II, pp 317–320. Kluwer Academic Publishing, Dordrecht, The Netherlands.
[26] Szalai, V.A. and Brudvig, G.W. (1996) Biochemistry 34, 1946–1953.
[27] Boussac, A. and Etienne, A.-L. (1982) FEBS Lett. 148, 113–116.
[28] Buser, C.A. and Brudvig, G.W. (1992) In Research in Photosynthesis (Murata, N., ed.), Vol. II, pp 85–88. Kluwer Academic Publishing, Dordrecht, The Netherlands.
[29] Beck, W.F., Innes, J.B., Lynch, J.B. and Brudvig, G.W. (1991) J. Magn. Res. 91, 12–29.
[30] Schweiger, A. (1991) Angew. Chem. Int. Ed. Engl. 30, 265–292.
[31] Britt, R.D., Zimmermann, J-L., Sauer, K. and Klein, M.P. (1989) J. Am. Chem. Soc. 111, 3522–3532.
[32] Eaton, S.S. and Eaton, G.R. (1995) J. Magn. Reson. 117, 62–66.
[33] Hansson, Ö., Aasa, R. and Vänngård, T. (1987) Biophys. J. 51, 825–832.
[34] dePaula, J.C., Li, P.M., Miller, A-F., Wu, B.W. and Brudvig, G. (1986) Biochemistry 25, 6487–6494.
[35] Berthomieu, C., Boussac, A., Maentele, W., Breton, J. and Nabedryk, E. (1992) Biochemistry 31, 11460–11471.
[36] Buser, C.A, Diner, B.A. and Brudvig, G.W. (1992) Biochemistry 31, 11441–11448.
[37] MacDonald, G.N., Boerner, R.J., Everly, R.M., Cramer, W.A., Debus, R.J. and Barry, B.A. (1994) Biochemistry 33, 4393–4400.

[38] Barry, B.A. and Babcock, G.T. (1990) J. Biol. Chem. 265, 20139–20143.
[39] Warncke, K., Babcock, G.T. and McCracken, J. (1994) J. Am. Chem. Soc. 116, 4332.
[40] Boussac, A. and Rutherford, A.W. (1995) Biochim. Biophys. Acta 1230, 195–201.
[41] Boussac, A., Girerd, J.-J. and Rutherford, A.W. (1996) Biochemistry 35, 6984–6989.
[42] Shen, J.-R. and Inoue, Y. (1991) Plant Cell. Physiol. 32, 453–457.
[43] Kusunoki, M. (1995) Chem. Phys. Lett. (1995) 239, 148–157.